Supplement of Earth Syst. Dynam., 17, 929–954, 2026
https://doi.org/10.5194/esd-17-929-2026-supplement

Earth System Dynamics
Open Access
EGU

Supplement of

Strong intensification of extreme fire weather in Europe under 3 °C compared to 2 °C global warming

A. Serkan Bayar et al.

Correspondence to: A. Serkan Bayar (serkan.bayar@ufz.de) and Alexandre M. Ramos (alexandre.ramos@kit.edu)

S1 Further Details on Bias Adjustment of EURO-CORDEX Model Outputs

Various methods have been developed for bias adjustment (Maraun, 2016), among which quantile-based univariate methods are arguably one of the most widely used. For this study, we selected the Quantile Delta Mapping (QDM) method (Cannon et al., 2015) to adjust the biases in the input fields from EURO-CORDEX simulations, which were then used to calculate the FWI. QDM is selected due to its ability to adjust biases in each quantile while preserving the relative change signal of the underlying climate model, as demonstrated for precipitation- and temperature-based indices (Cannon et al., 2015; Casanueva et al., 2020; Tong et al., 2021; Xavier et al., 2022). The fundamental QDM calculation procedure is given in the main text (see Section 2.2.1) with further details provided below.

Quantile-based methods can inherently correct the so-called drizzle effect, where models simulate too many rainy days compared to the reference data (Argüeso et al., 2013; Gutowski et al., 2003; Van de Velde et al., 2021), by multiplying the lower end of the distribution by zero. To address cases where modeled dry days are more frequent than in the reference data, Cannon et al. (2015) replaced dry days in both modeled and observed data with uniformly distributed non-zero values below a specified threshold prior to bias adjustment. After the bias adjustment, values below the threshold are returned to zero. This approach has later been referred to as Singularity Stochastic Removal (SSR) (Lehner et al., 2023; Vrac et al., 2016). SSR was applied here using a threshold of 0.05 mm day^{-1} to adjust occurrence biases in the EURO-CORDEX precipitation simulations, and a more conservative threshold of 0.1 mm day^{-1} was used to reset the values to zero after bias adjustment.

The biases in the seasonal cycle of each atmospheric field were adjusted using a three-month running window centered on the month of interest (Cannon et al., 2015). Future simulation periods were adjusted in separate 10-year batches to preserve climate change signals and reduce computational demands.

Table S1. FWI input combinations tested in this study to approximate the original noon-time FWI calculation.

Combination	Temperature	Precipitation	Relative Humidity	Wind Speed
Original	at noon	accumulated at noon	at noon	at noon
Comb-1	daily maximum	accumulated daily	daily mean	daily maximum
Comb-2	daily maximum	accumulated daily	daily mean	daily mean
Comb-3	daily maximum	accumulated daily	daily minimum	daily maximum
Comb-4	daily maximum	accumulated daily	daily minimum	daily mean

Table S2. Global warming level periods based on CMIP5 simulations. Thirty-year time periods depict when the specified global warming level relative to the preindustrial period is reached for the first time by the GCMs used as boundary conditions for the RCMs used in this study (scenario: RCP8.5). Note that each model follows a different trajectory to reach the relevant GWLs due to differences in climate sensitivity. For all simulations, preindustrial baseline period is 1881-1910, which is 0.46 °C colder than the reference period (1971-2000).

GCM	+2 °C GWL Period	+3 °C GWL Period
CNRM-CERFACS-CNRM-CM5	2029-2058	2052-2081
ICHEC-EC-EARTH	2028-2057	2052-2081
IPSL-IPSL-CM5A-MR	2020-2049	2039-2068
MOHC-HadGEM2-ES	2016-2045	2037-2066
MPI-M-MPI-ESM-LR	2029-2058	2052-2081
NCC-NorESM1-M	2031-2060	2057-2086

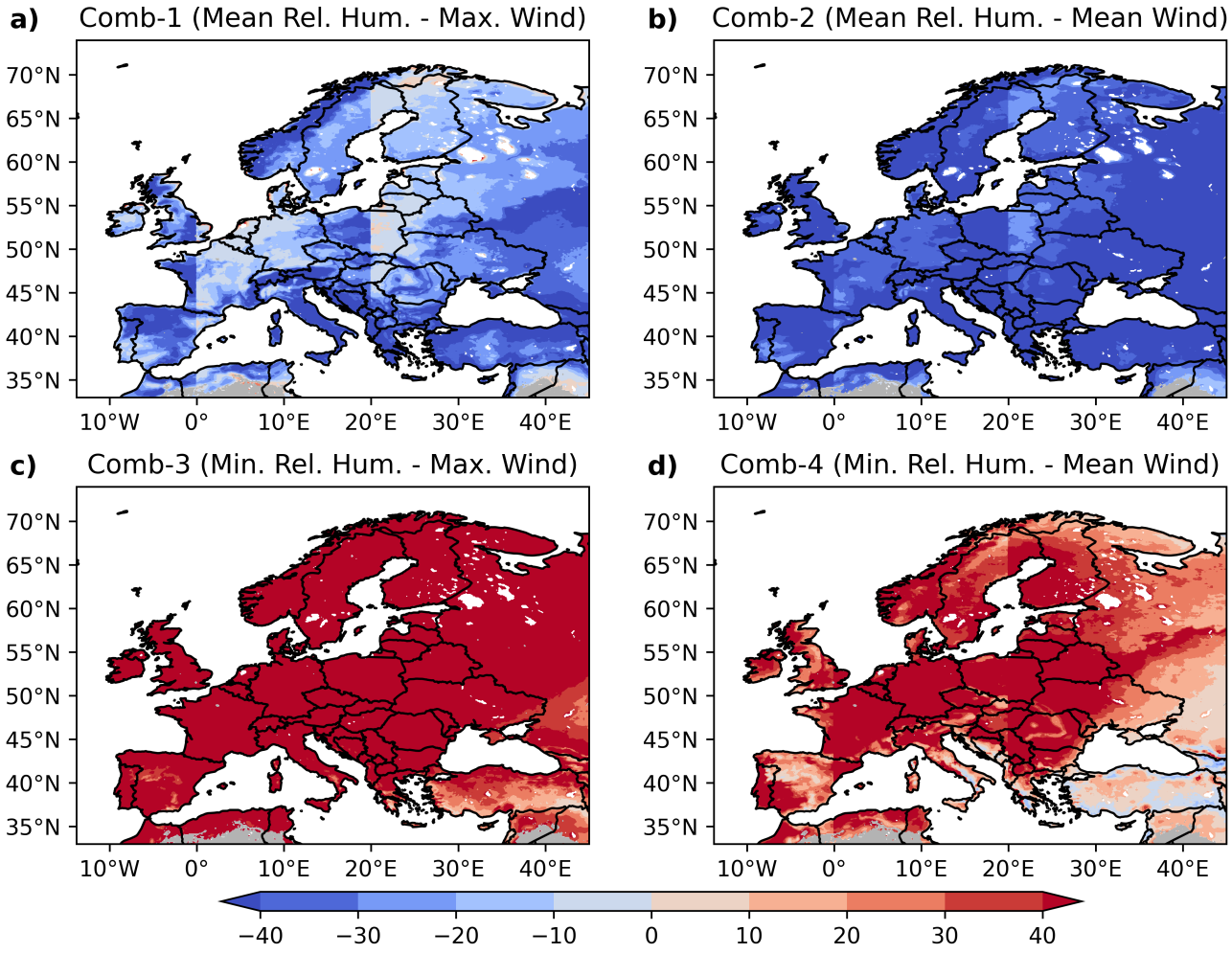

Figure S1. Relative percentage bias of the 50th percentile of FWI calculated using the four daily input variable combinations **a)** Comb-1, **b)** Comb-2, **c)** Comb-3, and **d)** Comb-4, compared to the original noon-time FWI calculation based on ERA5-Land reanalysis data. Daily maximum temperature and daily accumulated precipitation are common to all combinations. The time period analyzed is 1950-2023. Areas classified as unburnable are shown in gray. Note that the artifacts near 0° and 20° longitudes result from the concatenation operation described in Section 2.2.4 of the main manuscript. Details of the variables used in all combinations are given in Table S1.

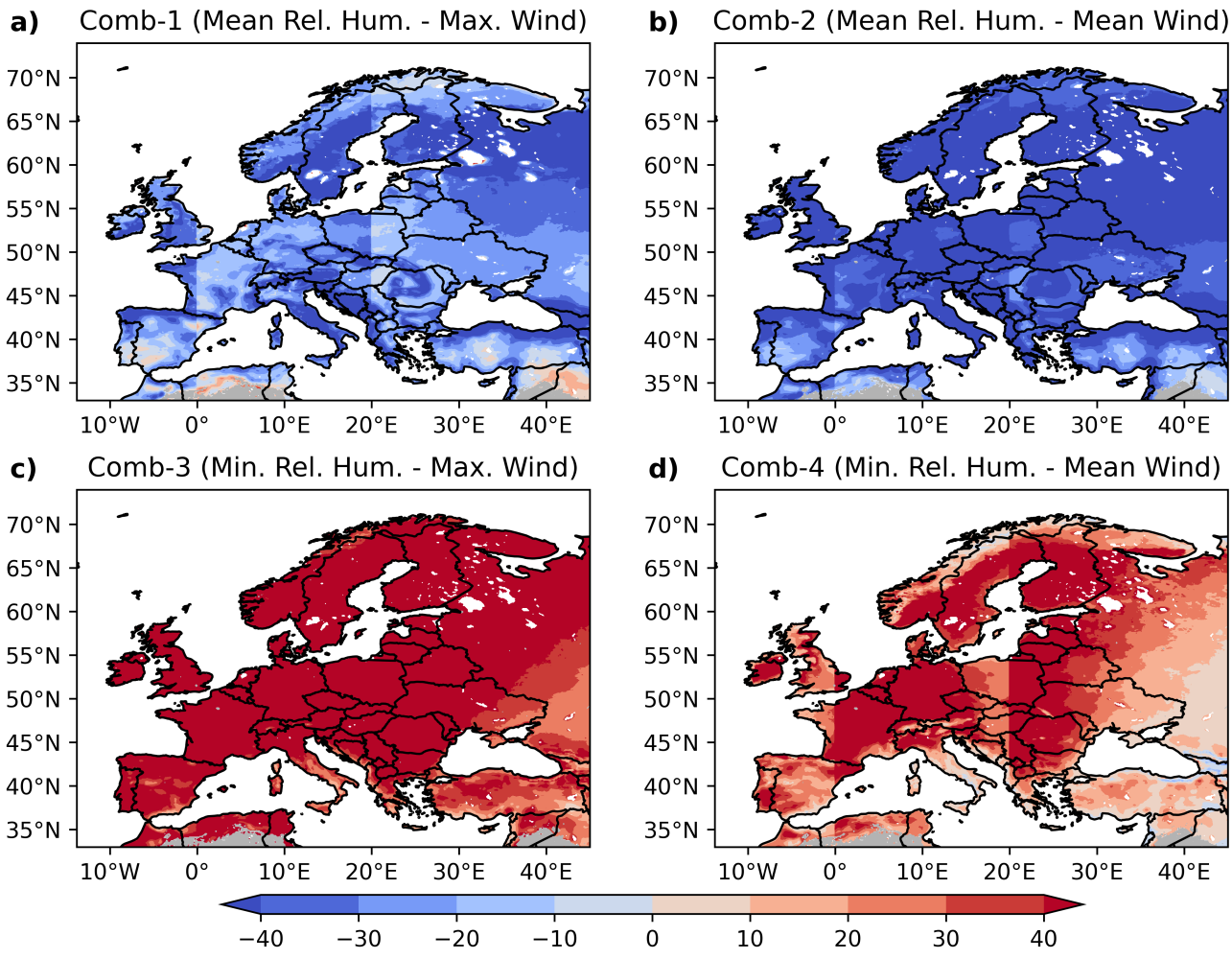

Figure S2. Same as in Figure S1, but for the 75th percentile.

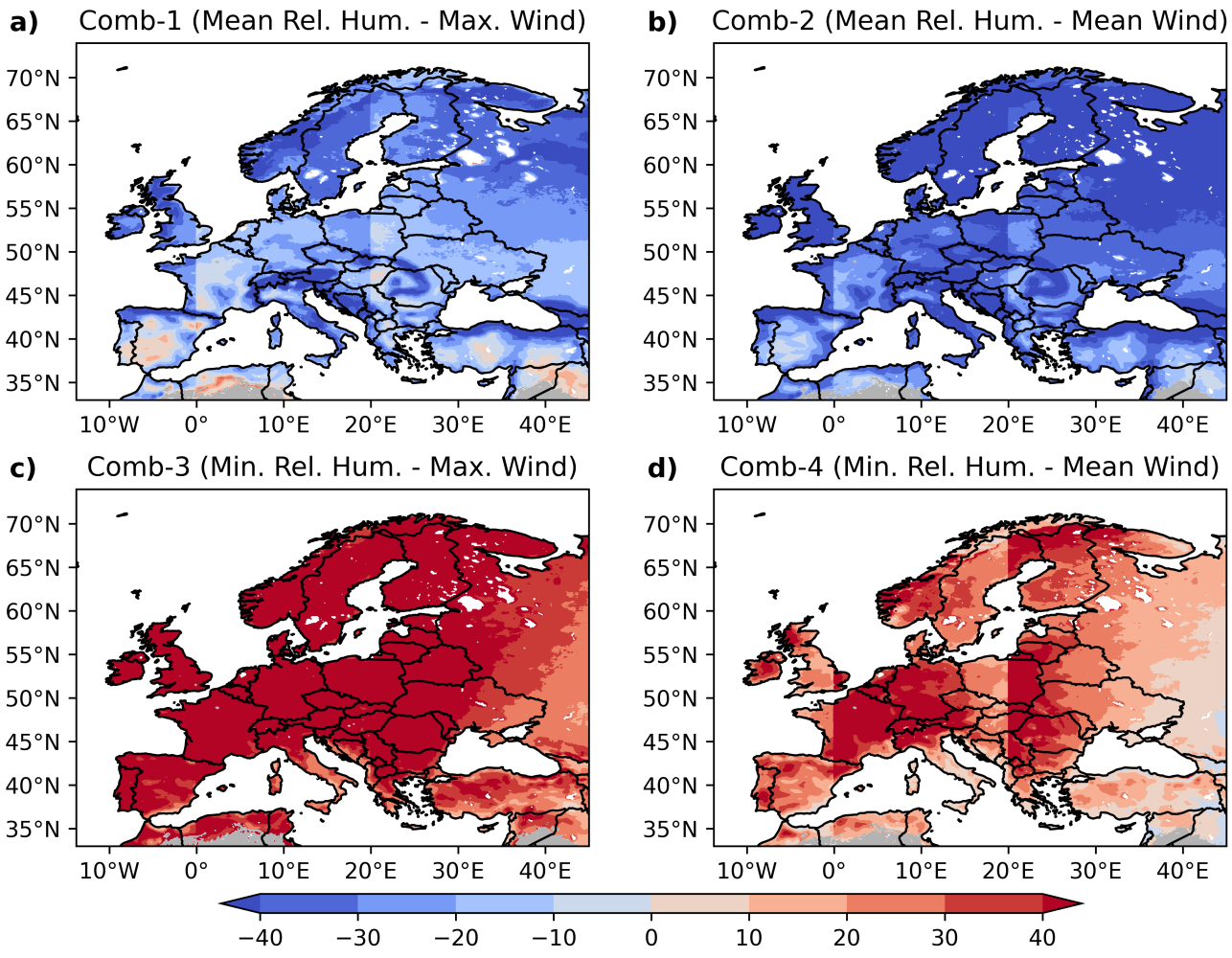

Figure S3. Same as in Figure S1, but for the 90th percentile.

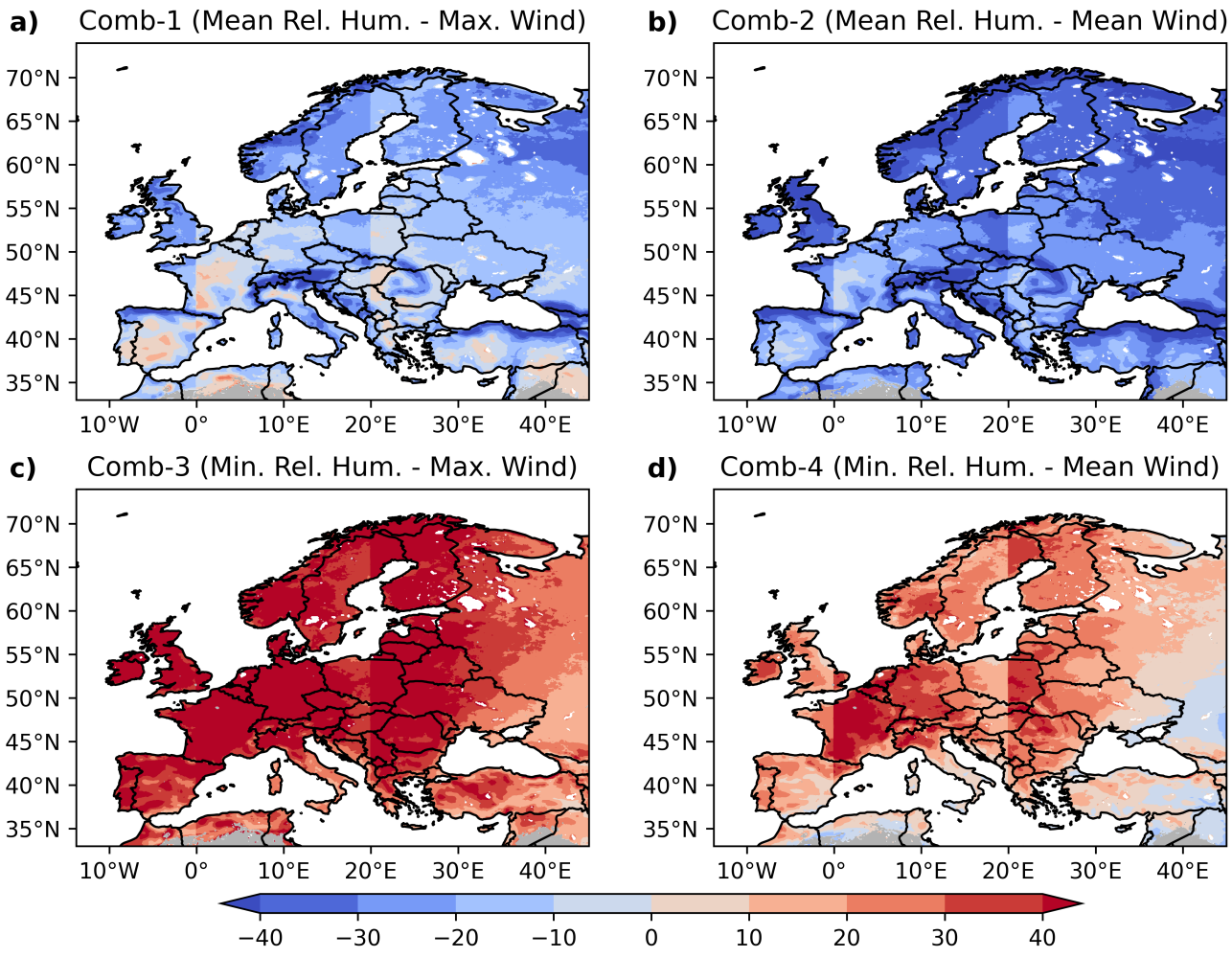

Figure S4. Same as in Figure S1, but for the 99th percentile.

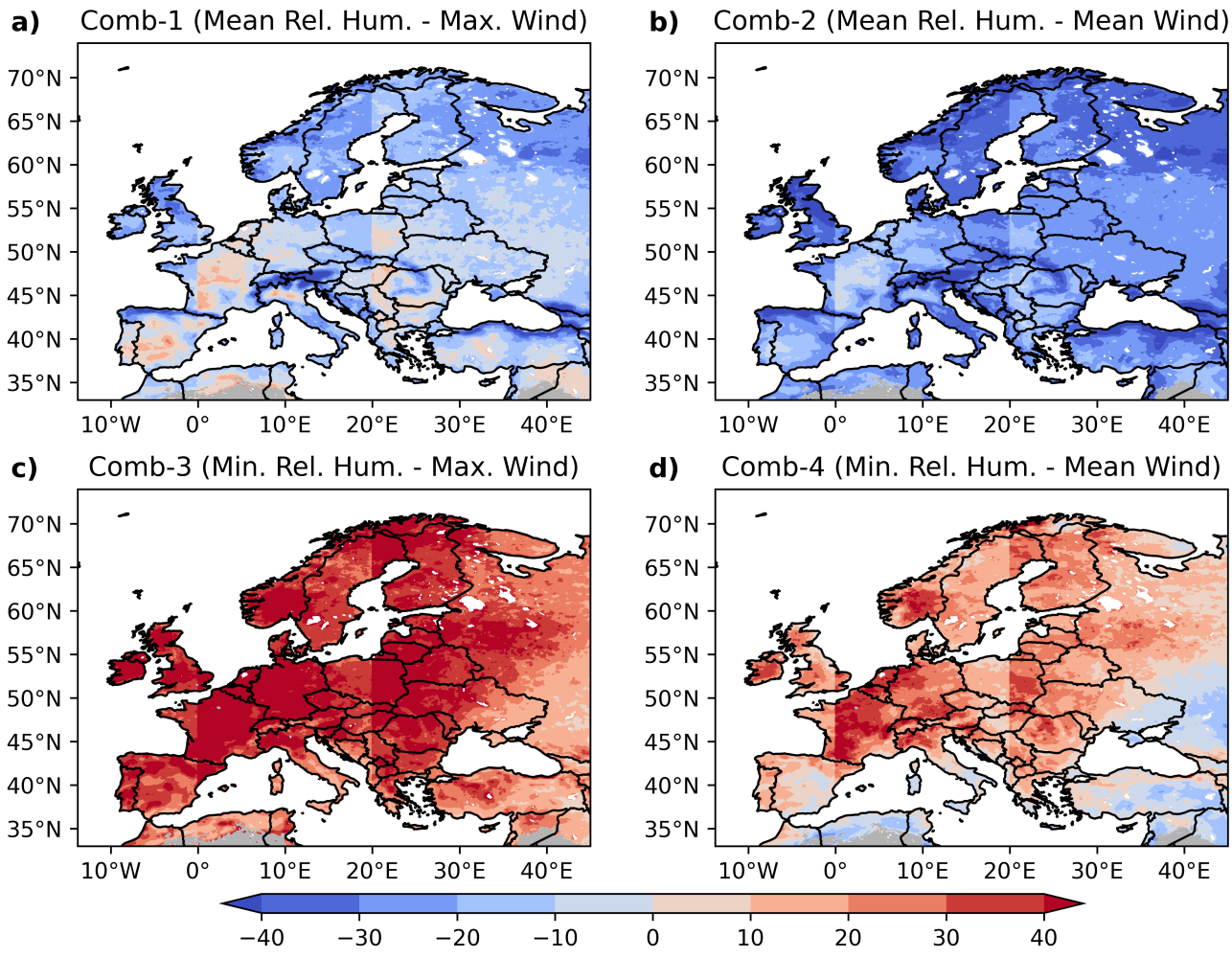

Figure S5. Same as in Figure S1, but for the 99.9th percentile.

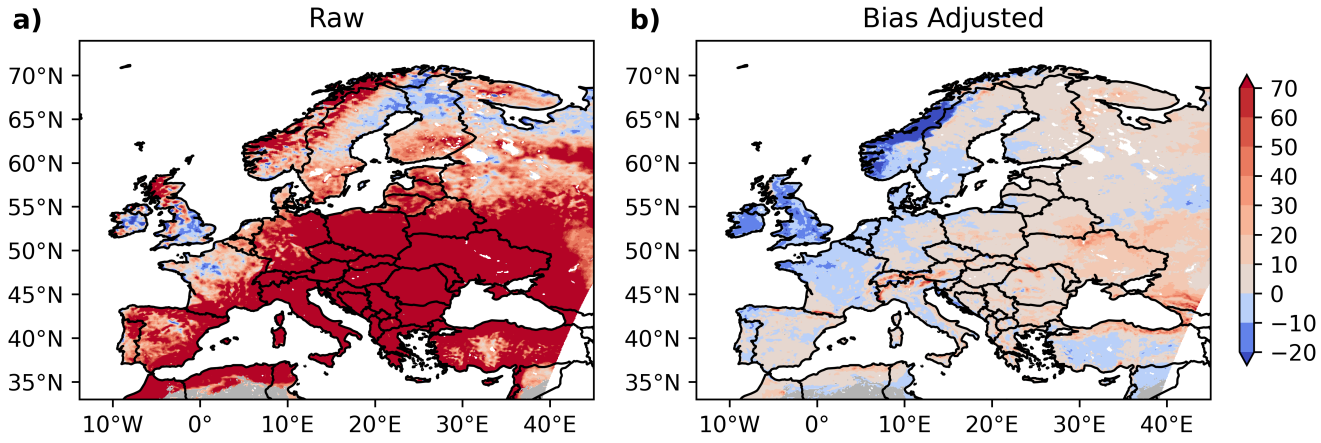

Figure S6. Relative percentage bias (%) in the 50th percentile of FWI for EURO-CORDEX ensemble median relative to ERA5-Land data during 1971-2000, based on **a)** raw (unadjusted) and **b)** bias-adjusted simulations. Areas classified as unburnable are shown in gray.

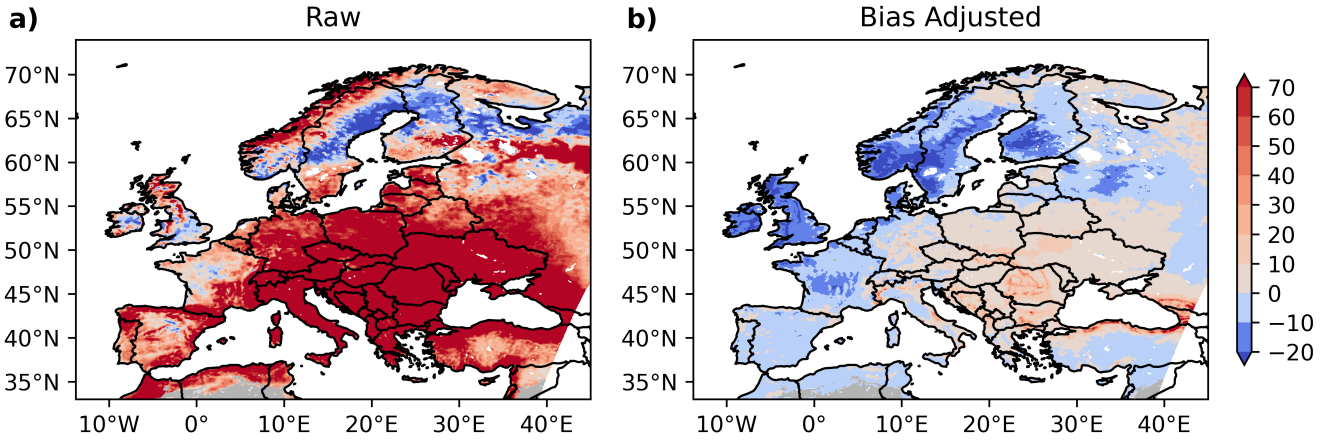

Figure S7. Same as in Figure S6, but for the 75th percentile.

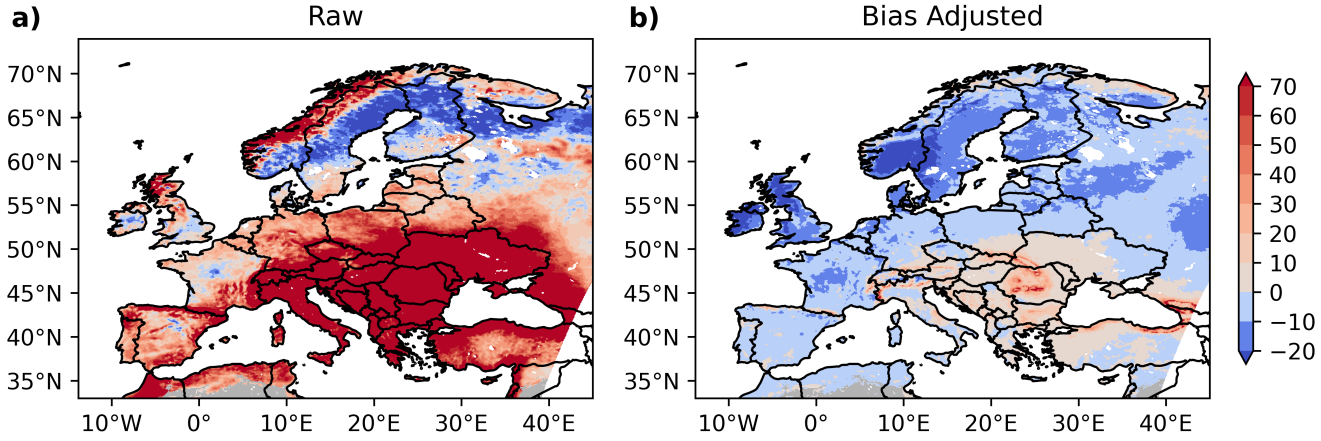

Figure S8. Same as in Figure S6, but for the 90th percentile.

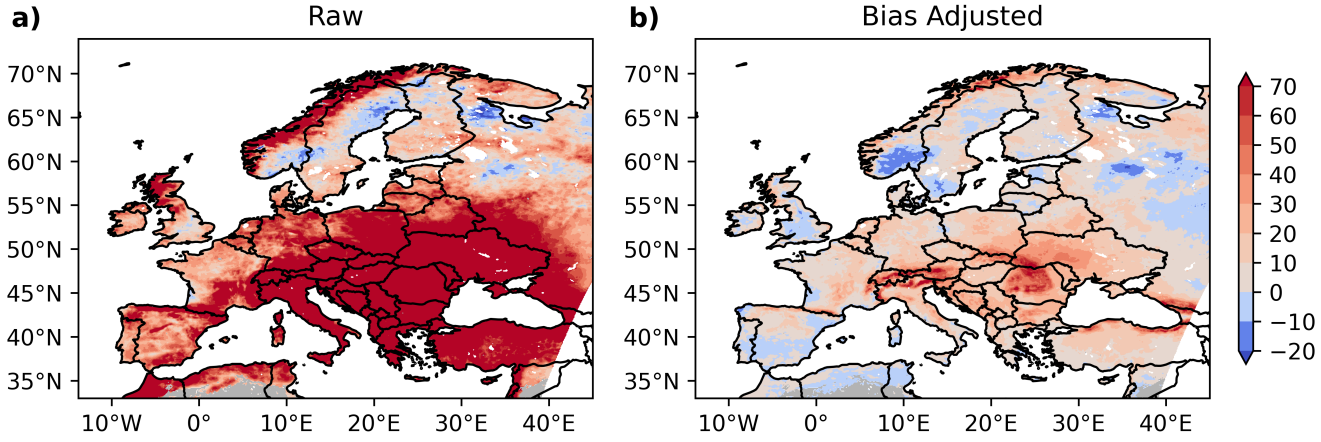

Figure S9. Same as in Figure S6, but for the 99th percentile.

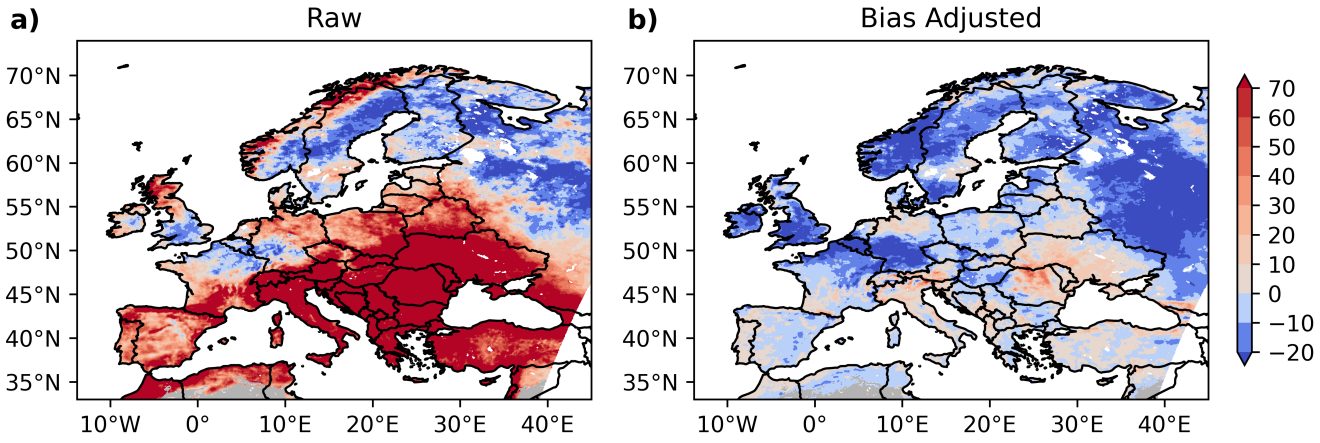

Figure S10. Same as in Figure S6, but for the 99.9th percentile.

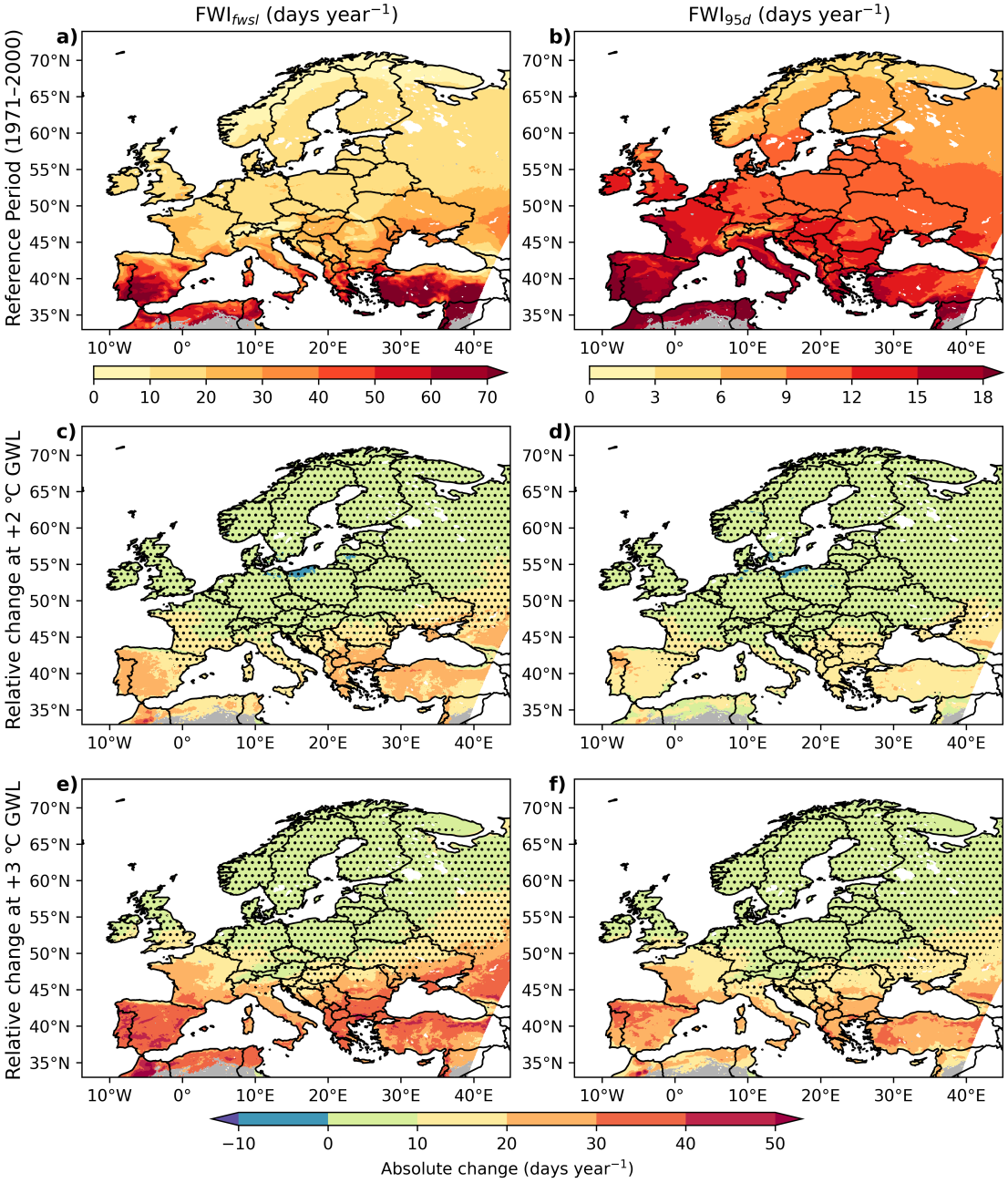

Figure S11. Patterns of frequency-based extreme fire weather metrics and their projected absolute changes in Europe based on the ensemble median of 33 bias-adjusted EURO-CORDEX models. The left panels show the fire weather season length (FWI_{fwsl}) and the right panels show the number of days per year exceeding the 95th percentile FWI (FWI_{95d}) relative to the reference period (1971-2000). **a, b)** Reference period patterns with a separate colorbar shown below, **c, d)** absolute changes relative to the reference period at +2 °C GWL and **e, f)** absolute changes relative to the reference period at +3 °C GWL. Note that the reference period is already 0.46 °C warmer than the preindustrial period. Areas without stippling indicate regions where at least 66% of the models project statistically significant changes according to a t-test ($p < 0.05$) and agree on the sign of change. Areas classified as unburnable are shown in gray.

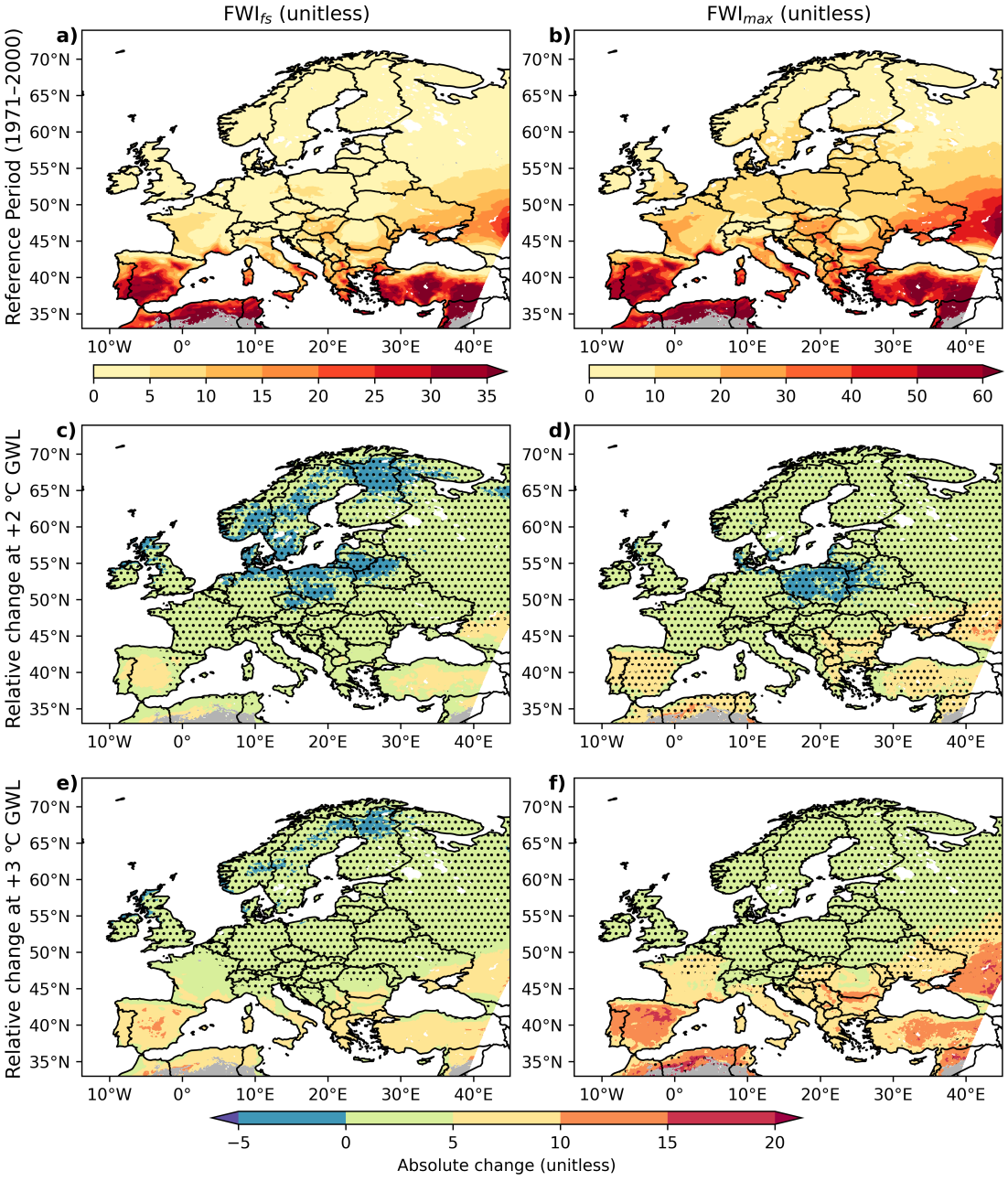

Figure S12. Patterns of magnitude-based extreme fire weather metrics and their projected absolute changes in Europe based on the ensemble median of 33 bias-adjusted EURO-CORDEX models. The left panels show the annual peak 90-day average FWI (FWI_{fs}) and the right panels show the annual maximum FWI (FWI_{max}). **a, b)** Reference period (1971-2000) patterns with a separate colorbar shown below, **c, d)** absolute changes relative to the reference period at +2 °C GWL and **e, f)** absolute changes relative to the reference period at +3 °C GWL. Note that the reference period is already 0.46 °C warmer than the preindustrial period. Areas without stippling indicate regions where at least 66% of the models project statistically significant changes according to a t-test ($p < 0.05$) and agree on the sign of change. Areas classified as unburnable are shown in gray.

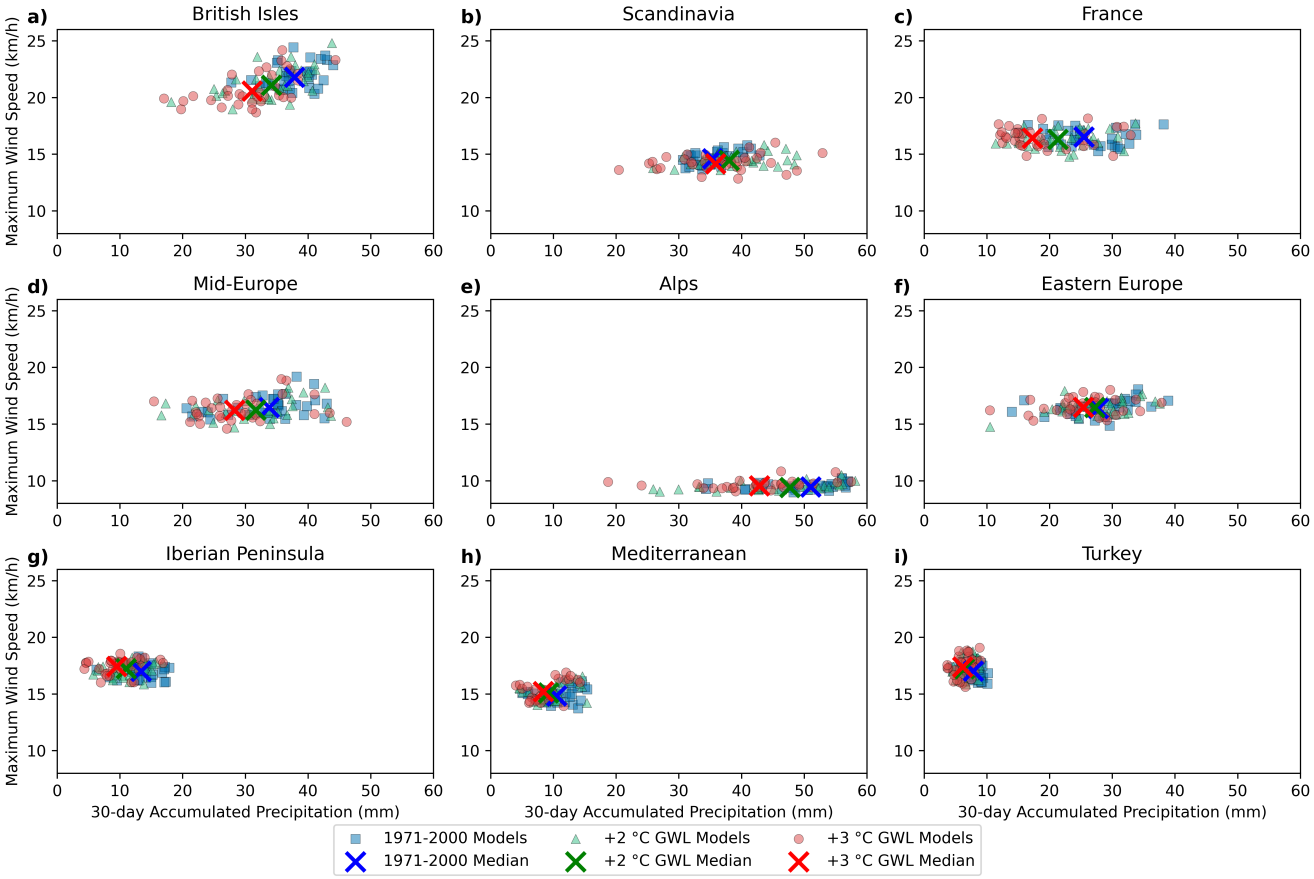

Figure S13. Accumulated 30-day antecedent precipitation (mm) vs. maximum wind speed (km/h) composites for the PRUDENCE regions. Accumulated precipitation and maximum wind speed averages are shown for days when the FWI exceeds its 99th percentile. Blue squares denote the reference period (1971-2000), green triangles correspond to 2 °C GWL, and red circles represent 3 °C GWL. All values are spatially aggregated and area-weighted averaged over the PRUDENCE regions, namely **a)** British Isles, **b)** Scandinavia, **c)** France, **d)** Mid-Europe, **e)** Alps, **f)** Eastern Europe, **g)** Iberian Peninsula, **h)** Mediterranean, and **i)** Turkey. Each value corresponds to a bias adjusted EURO-CORDEX model; crosses indicate ensemble medians.

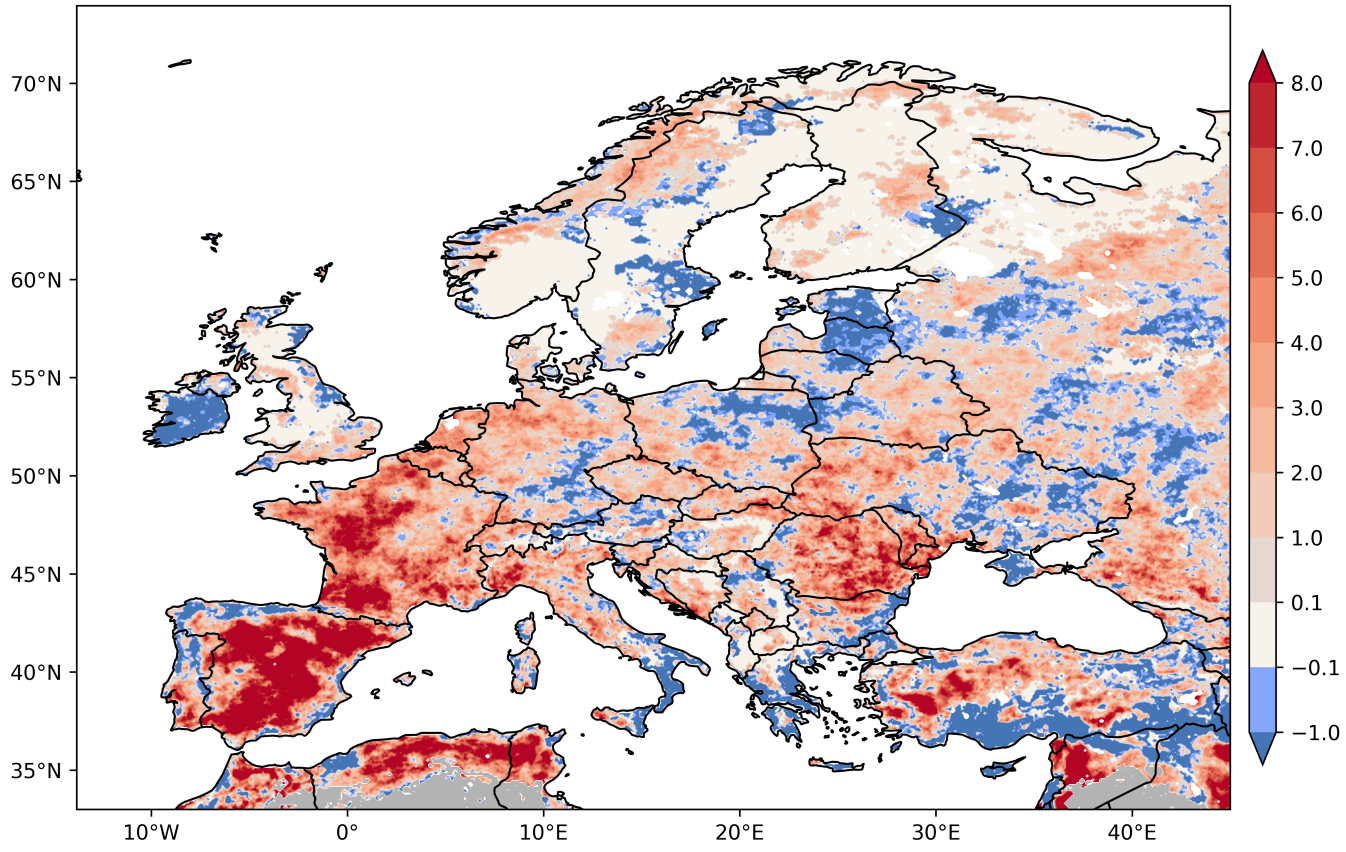

Figure S14. Spatial pattern of the relative difference between FWI_{95d} trends derived from the daily proxy-based FWI estimate and those derived from the original FWI calculation, expressed as a percentage of the original calculation, using ERA5-Land over the period 1950-2023. Positive values indicate that the daily proxy-based estimate overestimates the trend relative to the original calculation, while negative values indicate underestimation.

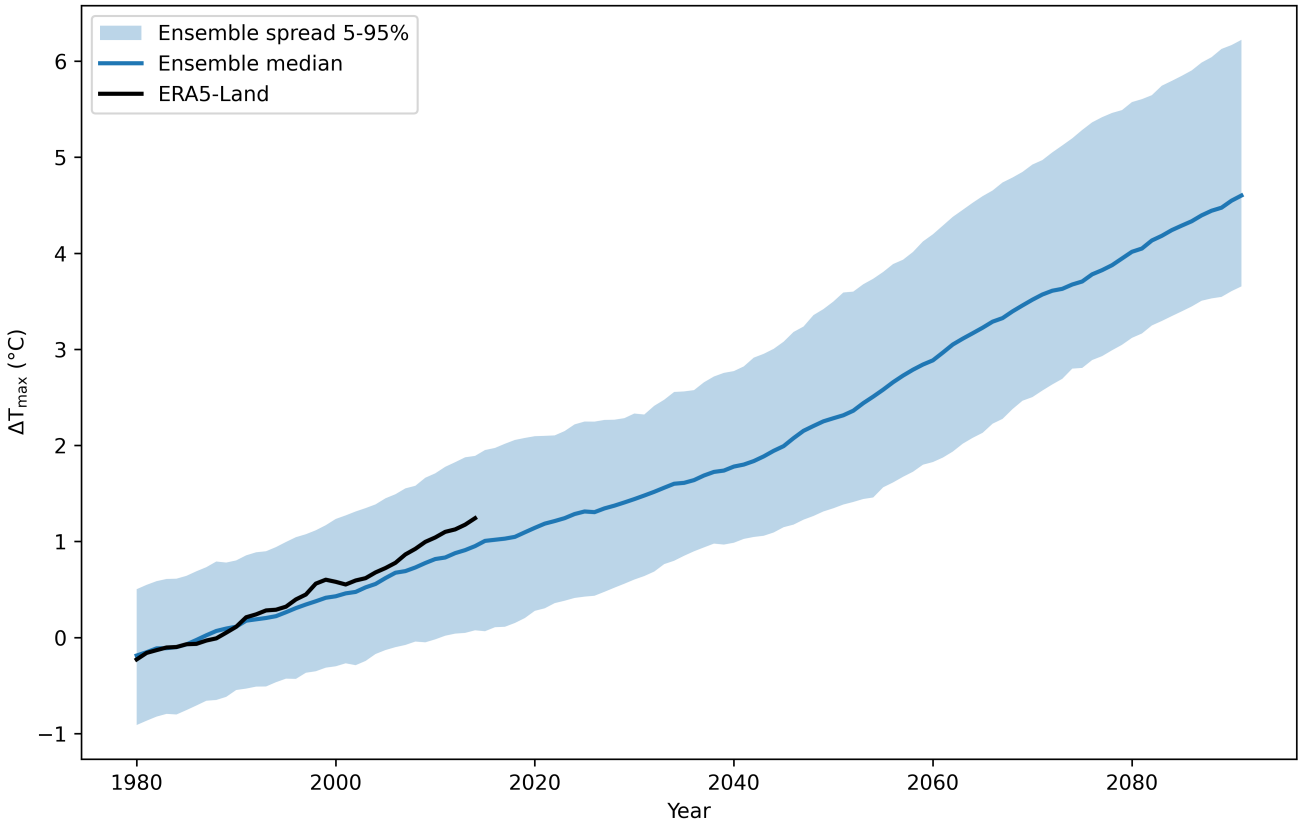

Figure S15. Annual mean daily maximum temperature from the EURO-CORDEX ensemble (blue) and ERA5-Land reanalysis (black), shown as anomalies relative to the reference period (1971-2000) and averaged over the study domain. Time series are presented as 20-year running averages to suppress high-frequency variability.

References

Argüeso, D., Evans, J. P., and Fita, L.: Precipitation bias correction of very high resolution regional climate models, Hydrology and Earth System Sciences, 17, 4379–4388, https://doi.org/10.5194/hess-17-4379-2013, 2013.

Cannon, A. J., Sobie, S. R., and Murdock, T. Q.: Bias Correction of GCM Precipitation by Quantile Mapping: How Well Do Methods Preserve Changes in Quantiles and Extremes?, Journal of Climate, 28, 6938–6959, https://doi.org/10.1175/JCLI-D-14-00754.1, 2015.

Casanueva, A., Herrera, S., Iturbide, M., Lange, S., Jury, M., Dosio, A., Maraun, D., and Gutiérrez, J. M.: Testing bias adjustment methods for regional climate change applications under observational uncertainty and resolution mismatch, Atmospheric Science Letters, 21, e978, https://doi.org/10.1002/asl.978, 2020.

Gutowski, W. J., Decker, S. G., Donavon, R. A., Pan, Z., Arritt, R. W., and Takle, E. S.: Temporal–Spatial Scales of Observed and Simulated Precipitation in Central U.S. Climate, Journal of Climate, 16, 3841–3847, https://doi.org/10.1175/1520-0442(2003)016<3841:TSOOAS>2.0.CO;2, 2003.

Lehner, F., Nadeem, I., and Formayer, H.: Evaluating skills and issues of quantile-based bias adjustment for climate change scenarios, Advances in Statistical Climatology, Meteorology and Oceanography, 9, 29–44, https://doi.org/10.5194/ascmo-9-29-2023, 2023.

Maraun, D.: Bias Correcting Climate Change Simulations - a Critical Review, Current Climate Change Reports, 2, 211–220, https://doi.org/10.1007/s40641-016-0050-x, 2016.

Tong, Y., Gao, X., Han, Z., Xu, Y., Xu, Y., and Giorgi, F.: Bias correction of temperature and precipitation over China for RCM simulations using the QM and QDM methods, Climate Dynamics, 57, 1425–1443, https://doi.org/10.1007/s00382-020-05447-4, 2021.

Van de Velde, J., Demuzere, M., De Baets, B., and Verhoest, N. E. C.: Exploring the Effect of Occurrence-Bias-Adjustment Assumptions on Hydrological Impact Modeling, Water, 13, 1573, https://doi.org/10.3390/w13111573, 2021.

Vrac, M., Noël, T., and Vautard, R.: Bias correction of precipitation through Singularity Stochastic Removal: Because occurrences matter, Journal of Geophysical Research: Atmospheres, 121, 5237–5258, https://doi.org/10.1002/2015JD024511, 2016.

Xavier, A. C. F., Martins, L. L., Rudke, A. P., de Morais, M. V. B., Martins, J. A., and Blain, G. C.: Evaluation of Quantile Delta Mapping as a bias-correction method in maximum rainfall dataset from downscaled models in São Paulo state (Brazil), International Journal of Climatology, 42, 175–190, https://doi.org/10.1002/joc.7238, 2022.